PASJ: Publ. Astron. Soc. Japan **54**, 33–38, 2002 February 25

Ram-Pressure Effects on Dense Molecular Arms in the Central Regions of Spiral Galaxies by Intracluster Medium

Makoto HIDAKA and Yoshiaki SOFUE
Institute of Astronomy, The University of Tokyo, Mitaka, Tokyo 181-0015
sofue@ioa.s.u-tokyo.ac.jp

(Received 2001 October 2; accepted 2001 December 6)

Abstract

We investigated ram-pressure effects by an intracluster wind on an inner disk of spiral galaxies by a hydrodynamical simulation. Even if the wind is mild and not strong enough to strip the gas disk, the ram pressure disturbs orbits of the inter-arm gas significantly. This results in asymmetric dense molecular arms in the inner few kpc region of a galaxy. This mechanism would explain the asymmetric CO gas distributions in the central regions often observed in Virgo spirals.

Key words: galaxies: cluster of — galaxies: ISM — galaxies: kinematics and dynamics — galaxies: spiral — intergalactic matter

1. Introduction

Ram-pressure by intracluster medium (ICM) causes the stripping of interstellar matter (ISM) from galaxies (Farouki, Shapiro 1980; Kritsuk 1984; Gaetz et al. 1987; Balsara et al. 1994; Sofue 1994; Quilis et al. 2000). It also produces a disturbed distribution of ISM in galaxies, such as head-tail H I structures as observed in Virgo galaxies (Cayatte et al. 1990; Vollmer et al. 2000, 2001; Phookun et al. 1993; Phookun, Mundy 1995). The ram-pressure effect has, thus, been discussed mainly in relation to H I gas stripping and outer disk structures. However, little attention has been paid to its effect on the inner molecular disk and arms. Only a few authors have discussed the ram effect on the spiral structure (Tosa 1994) and molecular clouds (Kenney et al. 1990; Sofue 1994).

Kenney et al. (1990) have shown that Virgo galaxies often exhibit asymmetric inner molecular disks. A recent high-resolution CO-line survey of Virgo cluster galaxies such as NGC 4254 and NGC 4654 (Sofue et al. in preparation) has revealed that some of them show a significant asymmetry of the inner molecular disks and arms. It is not clear if such an inner deformation of dense gas disks can be produced by ram pressure effect, which is thought to be the cause of their deformed H I envelops. Since these two galaxies have no massive companion that can disturb such inner disks, and they both show a head-tail H I outer structure (Phookun et al. 1993; Phookun, Mundy 1995), the inner deformation of molecular disks could also be due to the ram-pressure effect, while such an inner ram effect has not yet been investigated.

If the wind is very strong, such as assumed by Quilis et al. (2000) for the core of a rich cluster with an ICM density of $\sim 3\times10^{-3}\,\mathrm{atom\,cm^{-3}}$ and a wind velocity higher than $\sim 2000\,\mathrm{km\,s^{-1}}$, the ISM of any galaxies would be completely stripped. On the other hand, if the wind is mild, in such a case as for the Virgo cluster, where the ICM density is of the order of 10^{-3}–$10^{-4}\,\mathrm{atom\,cm^{-3}}$ and the velocity is $\sim 1000\,\mathrm{km\,s^{-1}}$, outer H I envelopes are deformed to produce head-tail structures (Vollmer et al. 2000, 2001). In current simulations, such as those by Vollmer et al., which were aimed at gas stripping and tailing of the outer H I disks, the detailed behavior of the inner disk gas inside $\sim 10\,\mathrm{kpc}$ was not well understood because of the insufficient resolution.

In the present paper, we consider a mild ICM wind, and discuss its effect on the inner disk gas based on 2D hydrodynamical simulations with a higher resolution than that aimed at outer H I stripping, as above. If we simply apply the ram-stripping condition to an azimuthally structure-less gas disk, the ram pressure would hardly affect the inner disk. However, if we consider a spiral structure with an arm-to-interarm density contrast, it may happen that the ram-pressure can affect the low-density interarm gas. We consider here the possibility that the ram-pressure can affect the dense molecular gas within the central few kpc region of spiral galaxies through disturbances of the orbits of inter-arm gas, even if the ICM wind is not strong enough to strip the disk gas.

2. Ram-Pressure Force on the Arm and Interarm Gases

The component of the ram force parallel to the galactic plane exerted by an intergalactic wind on a gas element is given by

$$f_{\mathrm{ICM}} \sim \rho_{\mathrm{ICM}} s \delta v^2 \cos\alpha \sin\alpha, \tag{1}$$

where ρ_{ICM} and ρ_{ISM} are the gas densities of ICM and ISM, respectively, s is the surface area of the element, and α is the angle between the wind direction and the galactic plane (Farouki, Shapiro 1980; Kritsuk 1984; Sofue 1994; Tosa 1994). The motion of the undisturbed ISM element is governed by the gravitational force, which is approximately equal to the centrifugal force,

$$f_{\mathrm{ISM}} \sim \rho_{\mathrm{ISM}} d\, s\, v_{\mathrm{rot}}^2 / R, \tag{2}$$

where d is the thickness of the gas disk, and R is the galactocentric radius of the element. Now, the ratio of f_{ICM} to f_{ISM} is given by

$$\eta \sim \frac{n_{\rm ICM}}{n_{\rm ISM}} \frac{R}{d} \left(\frac{\delta v}{v_{\rm rot}} \right)^2 \cos\alpha \sin\alpha, \quad (3)$$

where $n_{\rm ICM}$ and $n_{\rm ISM}$ are the number densities of hydrogen atoms of the ICM and ISM, respectively. If η exceeds unity, the ram force can disturb the ISM motion, while if it is smaller than unity, the ISM motion is little affected.

Let us consider the inner part of a galaxy at $R \sim 5\,$kpc with $d \sim 100\,$pc, rotating at $v_{\rm rot} \sim 200\,{\rm km\,s^{-1}}$. For an ICM wind with $n_{\rm ICM} \sim 10^{-4}\,{\rm H\,cm^{-3}}$, $V_{\rm ICM} \sim 10^3\,{\rm km\,s^{-1}}$, and $\alpha \sim 45°$, we obtain the ratio to be

$$\eta \sim 0.6 n_{\rm ISM}^{-1}\ [{\rm H\,cm^{-3}}]. \quad (4)$$

This relation implies that the ISM is stripped if $n_{\rm ISM} \ll 1\,{\rm H\,cm^{-3}}$, since the force perpendicular to the galactic plane is of the same order. We stress, however, that the relation indicates that the orbits of the gas within the disk plane is significantly disturbed if $n_{\rm ISM} \sim 1\,{\rm H\,cm^{-3}}$, even if the wind is not strong enough to strip the gas. This may indeed apply to the inter-arm ISM in the inner disk within a few kpc radius. On the other hand, high-density galactic shocked arms, where $n_{\rm ISM} \gg 1\,{\rm H\,cm^{-3}}$, would be hardly disturbed. We, thus, anticipate that, even if the ICM wind is mild, not strong enough to strip the disk, the interarm gas in the inner disk would be significantly disturbed, which may result in deformed galactic shock waves. Since δv is greater on the head-wind side of the rotation axis compared to the following-wind side, the deformed shock waves could be asymmetric with respect to the rotation axis.

Figure 1 illustrates the ram-deformation mechanism of the dense molecular arms, and how a lopsided spiral pattern is created. Since the density of the inter-arm gas (A and A′ in figure 1) is much lower than the average density of the disk, the ram force by the ICM wind (thin arrows) easily disturbs the orbits of inter-arm gas (thick curved arrows). The gas on the distorted orbits encounters density waves (dashed spirals) at different places (B and B′) from those expected for undisturbed orbits (dashed lines), and produces deformed dense molecular arms (thick spirals). In the next sections we discuss a numerical simulation of the ram deformation of spiral arms in order to understand whether this mechanism can indeed create deformed shocked arms, and how the deformed arms look like in realistic model disks.

3. Numerical Simulation

3.1. Basic Assumptions

The ram-pressure acceleration per unit mass is given by

$$\vec{a}_{\rm ram} = C n_{\rm ICM} \left| \vec{V}_{\rm ICM} - \vec{v}_{\rm rot} \right| \left(\vec{V}_{\rm ICM} - \vec{v}_{\rm rot} \right), \quad (5)$$

where $n_{\rm ICM}$ is the ICM density, $\vec{V}_{\rm ICM}$ is the ICM velocity with respect to the galaxy, $\vec{v}_{\rm rot}$ is the circular velocity of the clouds, and C is evaluated to be on the order of Σ^{-1} (e.g., Tosa 1994).

We assume that the galactic disk is thin and faces the ICM wind everywhere, being not shielded by neighboring clouds. Because this assumption would not apply to an edge-on wind, we consider here a wind with a mild inclination. We consider the inner disk of a galaxy, where the gravitational potential is deep and the ISM is dense enough so that stripping does not occur, as discussed in the previous section, and we treat a 2D disk in a fixed rotating potential.

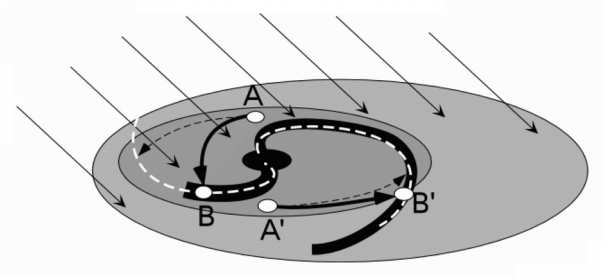

Fig. 1. Schematic illustration of the ram-deformation mechanism to cause asymmetric inner molecular arms. Orbits (thin dashed arrows) of low-density inter-arm gas (A and A′) are disturbed by the ram pressure of the ICM wind (thin arrows). The gas on the distorted orbits (thick arrows) encounters density waves (dashed spirals) at different places (B and B′) from those expected for undisturbed orbits (dashed spirals), and produces deformed dense gaseous arms (thick spirals).

For the velocity of a galaxy in the ICM $\vec{V}_{\rm ICM}$ and the ICM density $n_{\rm ICM}$, we adopt three values for each parameter. The galaxy's velocity, $\vec{V}_{\rm ICM}$, is taken to be 530, 1000, and $1500\,{\rm km\,s^{-1}}$, where the first value is suggested by Phookun and Mundy (1995) for NGC 4654 in the Virgo cluster. The ICM density, $n_{\rm ICM}$, is taken to be $1 \times 10^4\,{\rm H\,cm^{-3}}$, $5 \times 10^{-4}\,{\rm H\,cm^{-3}}$, and $1 \times 10^{-3}\,{\rm H\,cm^{-3}}$, where the first value is typical for the intergalactic density.

3.2. Numerical Method

For simplicity, we assumed that the interstellar gas is ideal, inviscid, and compressible. We used a freely downloadable and usable hydrodynamical code, VH-1 (Blondin, Lufkin 1993). This is a multidimensional hydrodynamics code for an ideal compressible fluid written in FORTRAN, developed by the numerical astrophysics group at the University of Virginia based on the Piecewise Parabolic Method Lagrangian Remap (PPMLR) scheme of Colella and Woodward (1984). The PPMLR has the advantage of maintaining contact discontinuities without the aid of a contact steepener, and is sufficiently good to be applied to a galactic-scale hydrodynamical simulation. The code does not take into account the gas's self-gravity, artificial viscosity, variable gamma equation of state, and radiative heating and/or cooling. The self-gravity of the gas is not taken into account, because we consider a case where the gas mass is not so much as to contribute to the density wave potential by the stellar disk, and also because we do not intend to discuss such processes as clumping of gas and cloud formation in the arm and inter-arm regions. The interstellar gas can be assumed to be isothermal, as is assumed here, while if cooling is taken into account, the shocked gas arms would become much denser than those calculated below. However, all such neglection would not affect the physical essence of the present study, which was aimed at simulating ram-deformation of the orbits of inter-arm gas and resulting disturbed shocked arms, as illustrated in figure 1.

3.3. Gravitational Potential

We implicitly give a gravitational potential, which comprises the following two terms: (i) a static axisymmetric potential, and (ii) a nonaxisymmetric, rotating bar potential. The potential is expressed by

$$\Phi(R,\phi) = \Phi_0(R) + \Phi_1(R,\phi). \tag{6}$$

We adopt a "Toomre disk" (Toomre 1981) potential for the axisymmetric component as given by

$$\Phi_0(R) = -\frac{c^2}{a}\frac{1}{(R^2+a^2)^{1/2}}, \tag{7}$$

where a is the core radius and $c = v_{\max}(27/4)^{1/4}a$. Through our numerical simulation, we fixd the core radius and maximum circular velocity to be $a = \sqrt{2}\,\mathrm{kpc}$ and $v_{\max} = 200\,\mathrm{km\,s^{-1}}$.

The nonaxisymmetric potential was taken from Sanders (1977), assuming rigid rotation at a pattern speed, Ω_p, which has the form

$$\Phi_1(R,\phi) = \varepsilon\frac{aR^2}{(R^2+a^2)^{3/2}}\Phi_0(R)\cos 2\left(\phi - \Omega_\mathrm{p}t\right), \tag{8}$$

where ε is the strength of the bar of the order of $\varepsilon = 0.15$. Spiral shocked arms of gas are produced by this potential.

3.4. Initial Conditions

Initially, we set 256×256 two-dimensional cells corresponding to $12.8\,\mathrm{kpc}\times12.8\,\mathrm{kpc}$ field, while setting the field center at the coordinates origin. The initial number density was taken to be $5\,\mathrm{cm^{-3}}$ the inner disk at $R \geq 8\,\mathrm{kpc}$ disk, and $1\,\mathrm{cm^{-3}}$ at $R > 8\,\mathrm{kpc}$. The initial rotation velocity of each gas cell was set so that the centrifugal force would balance the gravitation. The bar pattern speed, Ω_p, was taken to be $23\,\mathrm{km\,s^{-1}}$, and the strength of the bar ε was taken to be 0.10.

4. Ram-Pressure Deformation of Dense Molecular Arms

4.1. Deformation of Inner Spiral Structure

Figure 2 shows the result of a simulation including ram-pressure effects for the various parameter combinations, as described in the previous section. Both the ISM and spiral pattern rotate counterclockwise, and the ICM wind blows from left to right. The simulation shows that the orbits of the diffuse inter-arm gas are easily disturbed by the ram force, which results in a significant displacement of galactic shock waves from their undisturbed symmetric positions, as illustrated in figure 2.

Highly asymmetric dense spiral arms in the central region are produced by this mechanism if the wind speed is higher than $\sim 1000\,\mathrm{km\,s^{-1}}$ and the ICM density is greater than several $10^{-4}\,\mathrm{H\,cm^{-3}}$. A head-tail structure of dense gases slanted to the ICM wind, like NGC 4654 nucleus, can be produced by this mechanism, if $n_\mathrm{ICM}\times V_\mathrm{ICM}^2$ is greater than $\sim 3\times10^{12}\,\mathrm{cm^{-1}\,s^{-2}}$. One spiral arm on the downstream side is prominent, reproducing the lopsided arms, as observed in NGC 4254 and NGC 4654.

4.2. Deformed Molecular Arms

We then calculated the distribution of molecular fraction (Elmegreen 1993) corresponding to figure 2. The molecular fraction is defined by

$$f_\mathrm{mol} = \frac{\rho_{\mathrm{H_2}}}{\rho_\mathrm{HI}+\rho_{\mathrm{H_2}}} = \frac{2n_{\mathrm{H_2}}}{n_\mathrm{HI}+n_{\mathrm{H_2}}}, \tag{9}$$

where $\rho_{\mathrm{H_2}}$, ρ_HI, $n_{\mathrm{H_2}}$ and n_HI are the mass and number densities of molecular and H I gases, respectively. We used a method described by Sofue et al. (1995) and Honma et al. (1995) to calculate the galaxy-scale molecular fraction; they investigated molecular fronts in spiral galaxies using a phase-transition model proposed by Elmegreen (1993). In this model, the molecular fraction is determined by three parameters; the interstellar pressure, P, the UV radiation field, U, and the metallicity, Z. For U and Z, we adopted an exponential function of galactocentric radius, and calculated f_mol for corresponding gas pressure, P, which is determined by the gas density in each cell.

Figure 3 shows the result of a numerical simulation of the molecular fraction. The inner few kpc region is dominated by molecular gas, where the molecular fraction is as large as $\sim$ 70–90%. Also, the molecular fraction increases suddenly at the galactic shocks, which are already deformed from symmetric arms. Thus, the simulation has revealed that highly deformed inner molecular arms can be produced by ram-pressure disturbances on the inter-arm low-density regions.

4.3. Comparison with Observations and Wind Velocities

We now compare the results with H I and CO-line observations of the Virgo galaxies, NGC 4254 and NGC 4654. The heliocentric radial velocity of NGC 4254, $2407\,\mathrm{km\,s^{-1}}$, is about $1100\,\mathrm{km\,s^{-1}}$ different from that of NGC 4486 (M 87), the center of the Virgo cluster, $1282\,\mathrm{km\,s^{-1}}$ (de Vaucouleurs et al. 1991). Also, by comparing with the lopsided H I distribution of NGC 4254 (Phookun et al. 1993) and the ram pressure simulation on galaxies (Abadi et al. 1999), we can exclude the possibility of any face-on motion of NGC 4254. Assuming that NGC 4254's orbit is inclined by 45° from the line of sight, we may estimate the velocity of motion of NGC 4254 in the Virgo cluster as being $\sim 1500\,\mathrm{km\,s^{-1}}$. Then, the rotation velocity of NGC 4254 ($\sim 150\,\mathrm{km\,s^{-1}}$) is negligible compared to the wind velocity, so that the H I tail grows toward downstream. The location of a prominent spiral arm (Iye et al. 1982) and the direction of rotation are consistent with our numerical simulation. However, if we assume a slower wind velocity, e.g., on the order of, or smaller than, $\sim 750\,\mathrm{km\,s^{-1}}$, the simulation cannot reproduce the observed features.

Our simulation for moderate ICM velocity, which predicts an off-center bar of dense gas tilted toward the ICM wind, is consistent with the observations of NGC 4654 in H I (Phookun, Mundy 1995) and CO (Sofue et al. in preparation). Our simulations show that spiral arm in the upstream side becomes stronger than that in the downstream side. Considering the location of the prominent optical arm (Frei et al. 1996) and an elongation of the observed molecular bar and H I tail, we find that the direction of motion of NGC 4654 is toward the northwest, with a significantly high velocity compared to the velocity dispersion of the Virgo cluster. Taking it into account that the rotation velocity of NGC 4654 is relatively slow, the velocity of NGC 4654 in the Virgo cluster would be greater than $1000\,\mathrm{km\,s^{-1}}$, although the heliocentric radial velocity,

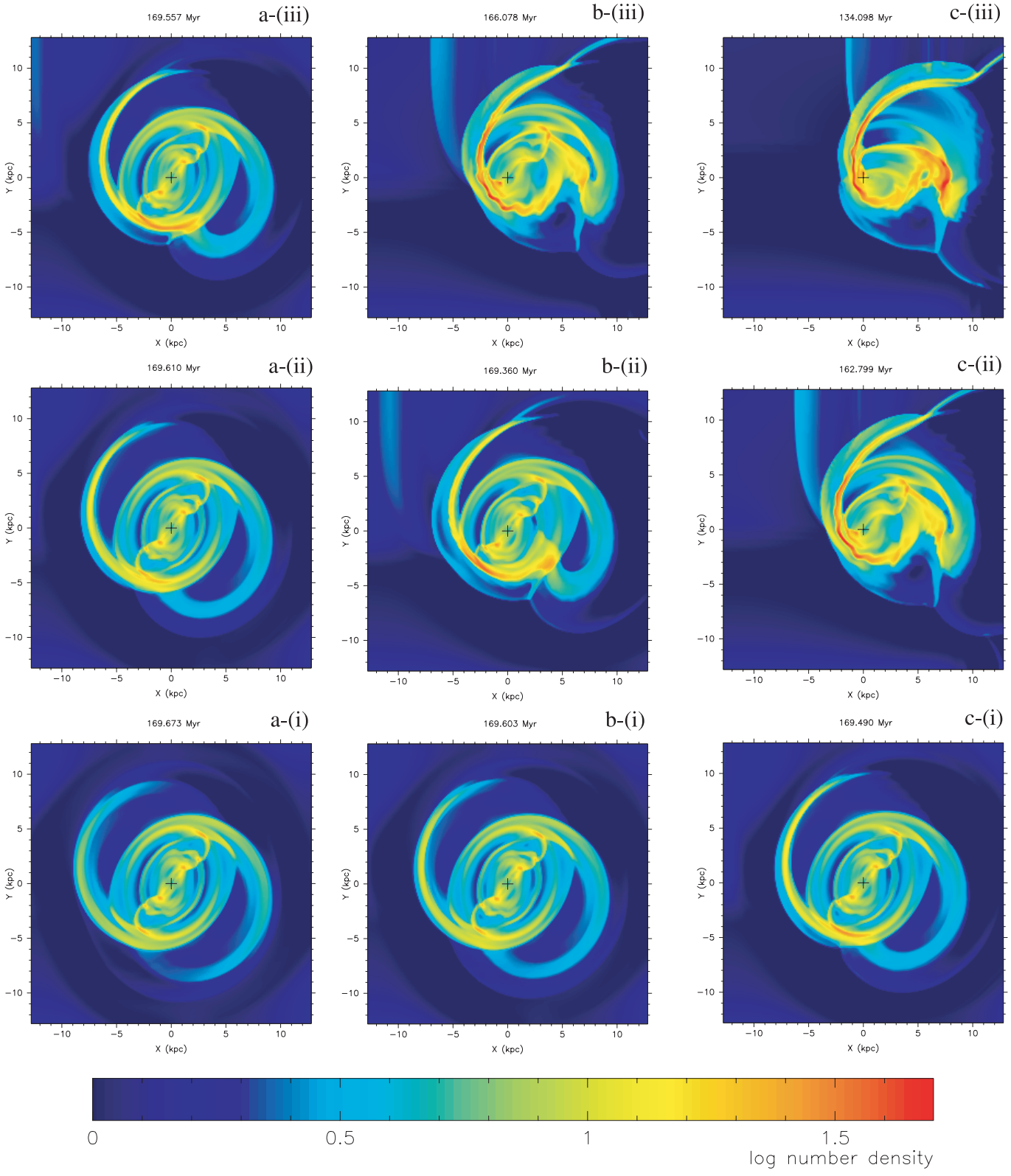

Fig. 2. Snapshots of the density distribution in the ram-pressure models after (1.3–1.7) $\times 10^8$ yr. The labels indicated the adopted parameters. Alphabets: ICM velocity, $\vec{V}_{\rm ICM}$ = (a) 530, (b) 1000, and (c) 1500 km s^{-1}. Roman numbers: ICM density $n_{\rm ICM}$ = (i)1 $\times 10^{-4}$, (ii) 5 $\times 10^{-4}$, and (iii) 1 $\times 10^{-3}$ cm^{-3}. The color-density key is shown at the bottom, which is common to all snapshots. The rotation direction of gases and a bar potential is counterclockwise, and ICM wind blows from left to right. The strength of the bar ε is 0.10 in all models. Weak straight waves toward upper and right boundaries in b-(ii, iii) and c-(ii, iii) are artifacts due to numerical reflections at the boundaries.

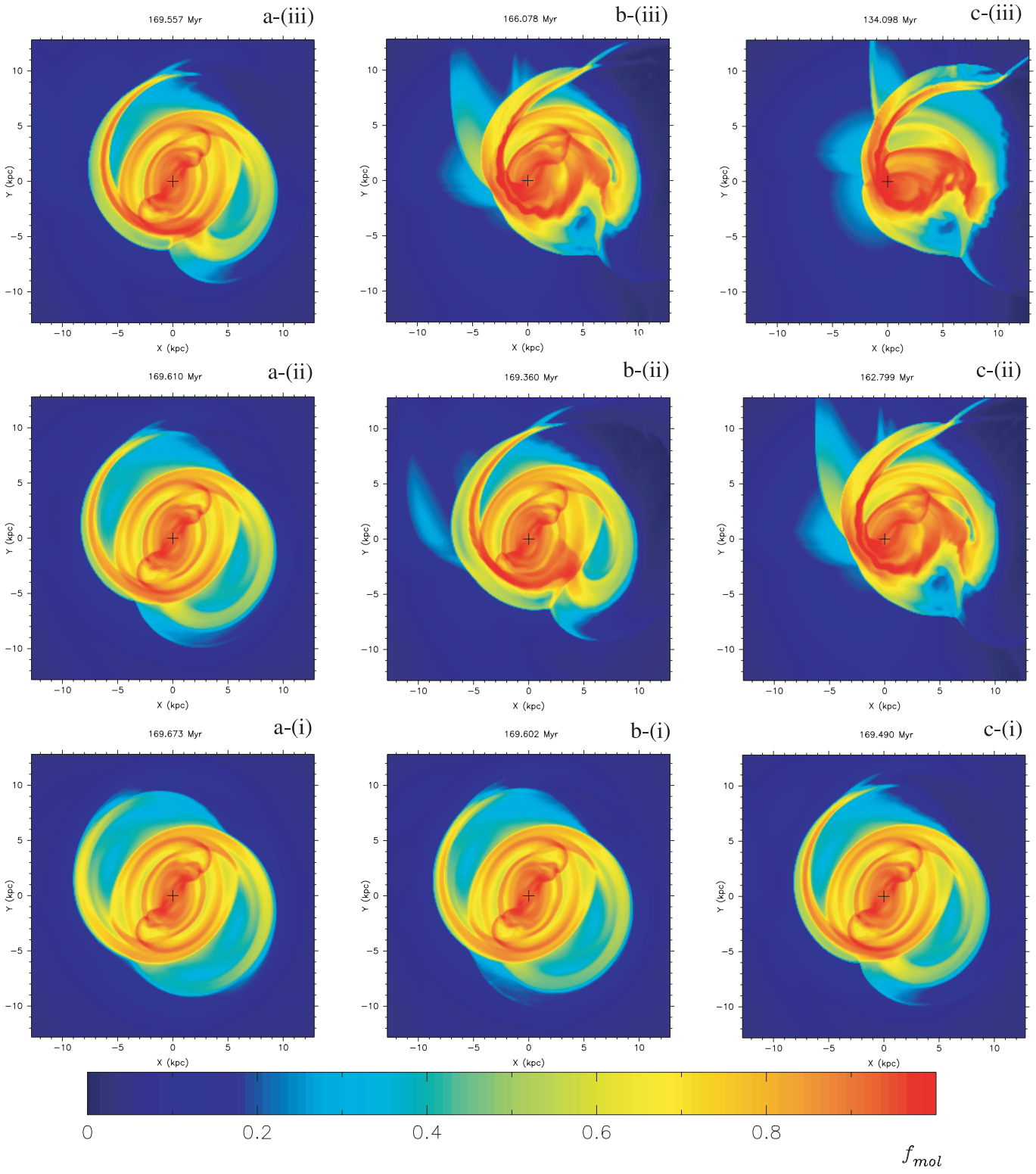

Fig. 3. Same as figure 2, but showing the distribution of molecular fraction, $f_{\rm mol}$.

$1054\,\mathrm{km\,s^{-1}}$, is close to Virgo's central velocity.

5. Discussion

We have considered the ram-pressure effects of a mild ICM wind on gaseous disks in cluster galaxies. Galaxies in the central region of the Virgo galaxies show H I deficiency, where the molecular gas fraction is higher than that of the galaxies in the outer region of the cluster (Kenney et al. 1990). This fact has been naturally explained by the ram-pressure stripping of the H I gas: the ram effects are negligible on the inner molecular disks, while it is crucial for the H I outer disk and envelops. On the other hand, it is also known that ram-affected Virgo galaxies show asymmetric CO gas distributions (Kenney et al. 1990; Sofue et al. in preparation).

In the present paper, we have shown that the orbits of the inter-arm ISM are disturbed by the ram pressure of the ICM wind, even if the wind is mild and not strong enough to strip the gas disk. The disturbed inter-arm ISM causes highly asymmetric molecular arms in the inner few kpc of the disk. The 3D simulation by Vollmer et al. (2000, 2001) for a similar wind condition shows that the inner disk within 10 kpc radius is not stripped, but suffers from perpendicular disturbances to the disk plane. Vertical displacements may result in off-plane molecular structure in the inner few kpc disk, in addition to the asymmetric arms as simulated here using the 2D scheme. Also, such 3D effects as the Kelvin–Helmholtz instability by the shearing motion between the disk and ICM (e.g. Mori, Burkert 2000) cannot be touched upon by the present 2D simulation. Therefore, detailed 3D simulations will be crucial to thoroughly understand the inner ram effect in more detail, while the present 2D results can tell us about some essential mechanism to cause the non-axisymmetric molecular structures in the inner disk.

However, in the cases of much stronger winds, the 2D assumption cannot be applied in any way, and 3D treatment of stripping is crucial. In fact, ram effect by a wind with a pressure much higher than that considered in this paper has been simulated by Quilis et al. (2000) with a 3D hydrodynamical simulation; they have shown that the ISM in a galaxy is completely stripped within one galactic rotation.

References

Abadi, M. G., Moore, B., & Bower, R. G. 1999, MNRAS, 308, 947
Balsara, D., Livio, M., & O'Dea, C. P. 1994, ApJ, 437, 83
Blondin, J. M., & Lufkin, E. A. 1993, ApJS, 88, 589
Cayatte, V., van Gorkom, J. H., Balkowski, C., & Kotanyi, C. 1990, AJ, 100, 604
Colella, P., & Woodward, P. R. 1984, J. Comp. Phys., 54, 174
de Vaucouleurs, G., de Vaucouleurs, A., Corwin, H. G., Jr., Buta, R. J., Paturel, G., & Fouqué, P. 1991, Third Reference Catalog of Bright Galaxies (New York: Springer-Verlag)
Elmegreen, B. G. 1993, ApJ, 411, 170
Farouki, R., & Shapiro, S. L. 1980, ApJ, 241, 928
Frei, Z., Guhathakurta, P., Gunn, J. E., & Tyson, J. A. 1996, AJ, 111, 174
Gaetz, T. J., Salpeter, E. E., & Shaviv, G. 1987, ApJ, 316, 530
Honma, M., Sofue, Y., & Arimoto, N. 1995, A&A, 304, 1
Iye, M., Okamura, S., Hamabe, M., & Watanabe, M. 1982, ApJ, 256, 103
Kenney, J. D. P., Young, J. S., Hasegawa, T., & Nakai, N. 1990, ApJ, 353, 460
Kritsuk, A. G. 1984, Astrophysics, 19, 263
Mori, M., & Burkert, A. 2000, ApJ, 538, 559
Phookun, B., & Mundy, L. G. 1995, ApJ, 453, 154
Phookun, B., Vogel, S. N., & Mundy, L. G. 1993, ApJ, 418, 113
Quilis, V., Moore, B., & Bower, R. 2000, Science, 288, 1617
Sanders, R. H. 1977, ApJ, 217, 916
Sofue, Y. 1994, ApJ, 423, 207
Sofue, Y., Honma, M., & Arimoto, N. 1995, A&A, 296, 33
Toomre, A. 1981, in The Structure and Evolution of Normal Galaxies, ed. S. M. Fall & D. Lynden-Bell (Cambridge: Cambridge Univ. Press), 111
Tosa, M. 1994, ApJ, 426, L81
Vollmer, B., Cayatte, V., Balkowski, C., & Duschl, W. J. 2001, ApJ, 561, 708
Vollmer, B., Marcelin, M., Amram, P., Balkowski, C., Cayatte, V., & Garrido, O. 2000, A&A, 364, 532